Available online at www.sciencedirect.com
SCIENCE DIRECT
Polymer 46 (2005) 6554–6562
polymer
www.elsevier.com/locate/polymer

Self-organized materials and graft copolymers of polymethylmethacrylate and polyamide-6 obtained by reactive blending

M. Freluche[a], I. Iliopoulos[a,*], J.J. Flat[b], A.V. Ruzette[a], L. Leibler[a]

[a]*Soft Matter and Chemistry (ESPCI-CNRS, UMR 7167), ESPCI, 10 rue Vauquelin, 75231 Paris, Cedex 05, France*
[b]*ARKEMA, CERDATO, 27470 Serquigny, France*

Available online 25 May 2005

Abstract

Nanostructured blends of poly(methylmethacrylate) and polyamide-6 (PMMA/PA6) were prepared by reactive blending. The grafting reaction occurs between the amino end-group of PA6 and glutaric anhydride units randomly distributed along the backbone of PMMA. Short PA6 grafts were used to facilitate reaction at the interface. Very fine morphologies were obtained after blending. Annealing the blends above the melting point of polyamide reveals that the amount of anhydride present on PMMA chains controls self assembly of the blends and stability of the copolymer at the interface. In some cases, stable swollen lamellar assemblies were achieved. These materials exhibit interesting properties such as transparency, creep resistance and solvent resistance.

Keywords: Reactive blending; Graft copolymer; Morphological stability

1. Introduction

Reactive blending is a well established route towards new materials from existing polymers [1]. In principle, it is possible to manufacture a large variety of materials starting from components that bear mutually reactive groups. During reactive blending, a copolymer is synthesized in situ at the interface. Block or graft architectures are obtained, depending on the location of the reactive groups on the polymers. These copolymers help to prevent coalescence and achieve homogeneous dispersion. Typically, a few weight percent of these copolymers is enough to stabilize micron-size dispersion. Recently, it has been shown that nanostructured blends can be obtained by a careful choice of molecular parameters of the components to enhance grafting at the interface [2–7]. However, some questions arise: are there rules to get stable dispersions upon annealing? What properties can be expected from self-assembly? In this work, we investigate these points through the study of PMMA/PA6 reactive blends.

The rate of grafting depends on the nature of the reactive groups and on the creation of new interface during blending. Some kinetic studies in the melt report that the order of reactivity is the same as in solution, implying that the fastest reaction is between anhydride and amine [8]. Note that this result was obtained for maleic anhydride and aliphatic amine. Other studies with the same model system report that the reaction rate increases as molecular weight decreases [9] and that the reaction depends on the location of reactive groups [10]. An end functional group reacts faster with another end-functional group than with a mid-functional one.

If the reaction is fast enough, the interface becomes quickly saturated with copolymer. Further grafting is mainly controlled by the residence time of the copolymer at the interface. Static annealing studies suggest that copolymers can leave the interface spontaneously (without shear) provided they are short enough [11–13]. This leads to higher conversion, especially if the polymers are shorter or close to their entanglement limit [4,12]. Pull-out, enhanced by shear, also depends on the architecture of the copolymer, linear copolymers being more easily expelled than grafted ones [3].

Taking these parameters into account, complete conversion of reactive units was achieved by Orr et al. on blends of 25,000 g/mol polymers of polystyrene and polyisoprene end-capped with anhydride and amine functions, respectively, [2]. Nearly pure multi-graft copolymer was further

* Corresponding author. Tel: +33 1 40 79 51 14; fax: +33 1 40 79 51 17.
E-mail address: ilias.iliopoulos@espci.fr (I. Iliopoulos).

0032-3861/$ - see front matter © 2005 Elsevier Ltd. All rights reserved.
doi:10.1016/j.polymer.2005.05.009

obtained by blending equal amount of poly(styrene-*co*-maleic anhydride) (SMA) and short polyamide-12 (average-number molecular weight from 1500 to 3000 g/mol) [5]. Increasing PA12 molecular weight to 15,000 g/mol dropped the reaction yield to only 24 mol% of PA12 grafted chains.

Nanostructured blends present high interest and can exhibit unique properties, including transparency. This occurs when remaining homopolymers are well incorporated in the self-assembly of the copolymer. Swelling of copolymer self-assemblies depends on the relative size of homopolymers and copolymer blocks and on the spontaneous radius of curvature of the copolymer [14–17]. Transparent materials containing 50 wt% of graft copolymer were obtained by Pernot et al. by blending a highly polydisperse maleinated polyethylene and short mono-aminated polyamide-6 [6]. The ratio of graft length to the distance between reactive groups along polyethylene backbone was chosen such as to favor large radii of curvature [18]. As a result, a bicontinuous structure was obtained. Natural disorder brought by polydispersity of polymer chains and randomness in grafts attachment enables local fluctuations of interface curvature and may further help swelling by homopolymers [6].

Here we propose to develop blends of PMMA and PA6. PMMA chains bear several intramolecular glutaric anhydride groups which have been found to be very reactive toward the amino end-group of PA6 [19]. We investigate the morphology of these blends as a function of the amount of reactive groups along the functionalized PMMA backbone. All investigated functionalized PMMA polymers have comparable molecular weight which means that the density of reactive units is the key parameter. A short PA6 is used here as the minor component. Post-blending annealing experiments were carried out to evaluate the interfacial behavior of the copolymer formed in situ. Properties of the resulting blends are also discussed.

2. Experimental section

2.1. Materials

Functionalized PMMA and mono-NH_2 terminated PA6 ($M_n = 2500$ g/mol, polydispersity index = 2), designated hereafter as PA, were provided by ARKEMA. Functionalized PMMA, designated as f-PMMA, bear carboxylic acid and dimethylglutaric anhydride groups randomly distributed along their backbone (Fig. 1). Three different f-PMMA were used, they are referred as PMMA**1**, PMMA**2** and PMMA**3**. Their characteristics are listed in Table 1. For the sake of comparison, blends were also prepared with a non-reactive PMMA, designated as PMMA**0**, provided by ARKEMA.

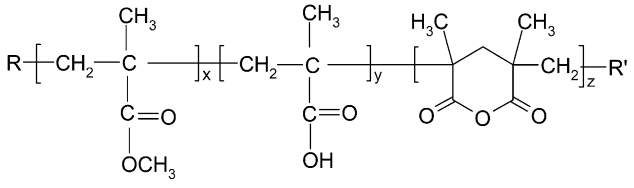

Fig. 1. Formula of functionalized PMMA.

2.2. Blend preparation

Blends of different compositions ranging from 80/20 to 60/40 (wt/wt) were prepared in a 3 g capacity co-rotating twin-screw micro-extruder (DACA Instrument). A feedback channel permits cyclic extrusion of the melt and is used to fix blending time. The two polymers were introduced simultaneously at 220 °C and blended at 60 rpm under N_2 atmosphere during 10 min.

Under the blending conditions, several reactions can occur besides the anhydride/amine grafting reaction. The functionalized PMMA used here bear methacrylic acid units which can react with their neighbor, either acid or ester, to give additional anhydride units [20]. The extent of this reaction was determined by extruding f-PMMA alone under the same conditions as the blends. A slight increase in anhydride fraction (on average 0.4 mol%) was measured and has been taken into account in the values listed in Table 1. Some grafting may also occur by direct reaction between acid groups of f-PMMA and amine groups. However, this reaction is very slow compared to the anhydride/amine one [8] and thus, grafting via amide bonds will be neglected with respect to grafting via imide bonds.

2.3. Blend characterization

Transmission Electron Microscopy was used to study the morphology of the blends. Ultrathin sections (ca. 60 nm thick) were microtomed from the extrudates at room temperature with a diamond knife and collected on gold grids. Polyamide was then selectively stained with phosphotungstic acid (30 min, 60 °C). Imaging was done on a ZEISS electron microscope operated at 100 kV.

The evolution of storage modulus and tan δ as a function of temperature were measured by dynamic mechanical analysis (DMA) using a TA Instrument DMA 2980 apparatus. Rectangular specimens ($5 \times 5 \times 1.5$ mm) melt-pressed at 225 °C were tested with a 2-point bending clamp (amplitude = 20 μm, $\nu = 1$ Hz, 2 °C/min). Glass transitions were taken at the maxima of tan δ.

Differential scanning calorimetry (DSC) measurements were performed on a TA Instrument DSC Q1000 apparatus to study crystallization of polyamide in the blends. Sample weight was about 10 mg. The temperature cycle consisted in a first heating from room temperature to 240 °C, then a cooling from 240 to 0 °C and a second heating from 0 to 240 °C. A rate of 5 °C/min was applied for this cycle. The degree of crystallinity was determined during the second heating, taking for reference the enthalpy of melting of a

Table 1
Characteristics of functionalized PMMA

Polymer	M_n[a] (g/mol)	M_w[a] (g/mol)	Anhydride[b] (mol%)	Acid[b] (mol%)	T_g (°C)[c]
PMMA**0**	24,000	51,000	0	0	132
PMMA**1**	48,000	102,000	0.5	4.0	156
PMMA**2**	42,000	84,000	5.7	2.2	154
PMMA**3**	40,000	83,000	7.5	1.5	162

[a] Measured by SEC in THF (universal calibration).
[b] Obtained by FTIR in chloroform.
[c] Corresponds to the maximum of tan δ measured by DMA.

PA6 100% crystallized in the α phase [21]. Using this procedure, no significant differences were observed between the extruded blends and the annealed samples.

The extent of reaction was determined by selective extraction of unreacted f-PMMA chains, performed with a soxhlet extractor in chloroform for 48 h. Extractions were performed on ca. 5 g of samples and repeated three times for some blends. The confidence interval for the evaluation of the amount of grafted f-PMMA was evaluated at $\pm 5\%$.

Solubility of the blends in a good solvent for PMMA was studied by immersing a piece of extrudate in chloroform, a non solvent for PA, for at least 72 h at room temperature.

3. Results

3.1. Morphology of the extrudates

Morphology of the as prepared blends is discussed first. Three preliminary observations evidence effective grafting between f-PMMA and PA during blending. First, there is a substantial increase in the torque measured on the micro-extruder just after the introduction of both components. Second, the materials obtained are quite transparent, especially those based on PMMA**2**. Finally, blending of PMMA**0** with PA leads to opaque extrudates and the torque remains constant. We will now focus on blends with 20 wt% of PA to compare the efficiency of the different f-PMMA backbones. Morphologies of the f-PMMA/PA 80/20 blends cut perpendicularly to the flow direction are displayed in Fig. 2(A)–(C). PA appears black and PMMA white on the TEM micrographs. In each blend, a very fine dispersion of polyamide is achieved, although the nodules of PA are not ordered and do not have a well defined shape. Blends of PMMA**2** and PA exhibit aggregates with an average mean diameter close to 15 nm whereas nodules in blends of PA with either PMMA**1** or PMMA**3** present a broad size distribution but remain smaller than 100 nm. The morphologies displayed in Fig. 2(A)–(C) are obviously strongly influenced by the shear applied during blending.

The fraction of grafted f-PMMA, determined by selective extraction, is listed for each blend in Table 2. Note that ungrafted PA chains could not be separated from the graft copolymer. Table 2 lists the composition of the blends in terms of fraction of unreacted f-PMMA homopolymer and graft copolymer plus unreacted PA chains. As suggested by the observed morphologies, the highest amount of grafted f-PMMA corresponds to the blend with PMMA**2**. There are indeed only 28% of ungrafted PMMA**2** in this blend against 48 and 60% for the blends based on PMMA**1** and PMMA**3**, respectively. The same optimum, as a function of f-PMMA functionality, was found for blends richer in PA (70/30 and 60/40, see Table 2).

The amount of grafted f-PMMA was also plotted as a function of the content of PA in the blend to evidence the trend for each f-PMMA (Fig. 3). The data corresponding to the 60/40 and 70/30 PMMA**3**/PA blends are not plotted, as the amount of grafted f-PMMA is overestimated in theses cases [22]. When the density of reactive units on f-PMMA is constant, an increase of PA content in the blend results in a higher amount of grafted f-PMMA chains. Thus, when PMMA**2** is blended with 40 wt% PA, almost all PMMA**2** is grafted. Steurer et al. observed the same trend for blends of SMA and PA12 and showed that the optimum of grafting of amine groups corresponds to equal amounts of SMA and PA12 [5]. They conjecture that when the PA fraction increases, more interface is available and the grafting reaction is thus more efficient.

The results reported so far suggest that grafting is optimum for PMMA**2** with an intermediate density of reactive groups.

3.2. Morphological stability

Samples were annealed above the melting point of PA at 225 °C under vacuum and cooled slowly (1 °C/min) to room temperature. On Fig. 2(D)–(F), morphology of the f-PMMA/PA blends after 20 h of annealing are compared to the ones obtained prior to annealing. Some extra grafting may occur during annealing. However, this additional grafting is minor compared to the extent of grafting reached during blending and should not affect self-assembly of the blends [23].

Very different behaviors are observed depending on the density of reactive groups on f-PMMA. First, annealing does not induce strong reorganization for the 80/20 PMMA**1**/PA blend: part of the aggregates observed in Fig. 2(A) tends to reorganize into rods, some coalescence occurs but the interface remains curved towards PA (Fig. 2(D)). In

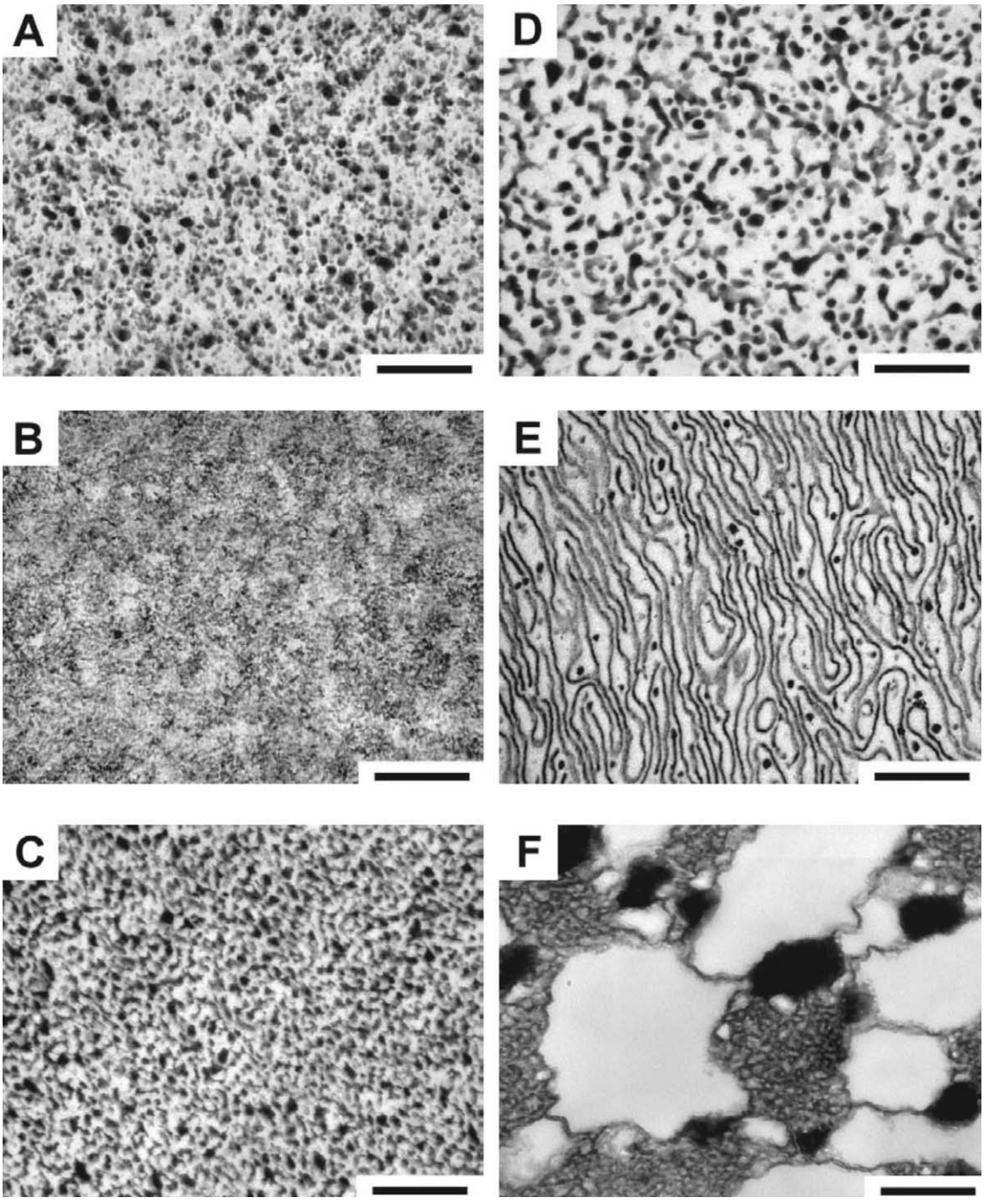

Fig. 2. TEM micrograph of the different 80/20 f-PMMA/PA blends at the end of the blending process and after 20 h of annealing at 225 °C (sliced perpendicular to the flow direction): (A) PMMA**1**, (B) PMMA**2** and (C) PMMA**3** blends prior to annealing and (D) PMMA**1**, (E) PMMA**2** and (F) PMMA**3** blends after annealing. The scale corresponds to 500 nm.

the 80/20 PMMA**2**/PA blend, PA sheets form upon annealing (Fig. 2(E), see also Fig. 4(A) for a higher magnification). In this case, self-assembly tends to favor a flat interface and only a few PA aggregates are observed (dark spots). In contrast, annealing induces macroscopic phase separation of the PMMA**3**/PA blend into a graft copolymer-rich phase and two homopolymer-rich phases (Fig. 2(F)). PMMA**3**-rich domains are around 1 μm big and free PA domains are located on the boundary of PMMA**3** and graft copolymer-rich domains and range from approximately 100 to 500 nm in size. Such reorganizations are obvious even for short times of annealing, for instance 30 min (data not shown).

The same trend as a function of PMMA functionality is observed for the blends containing higher amounts of PA. For instance, the evolution of the morphology as a function

Table 2
Main characteristics of the blends

Blend composition f-PMMA/PA	Matrix	Extrudate composition		Relative amount of grafted f-PMMA[a]	Degree of crystallinity of PA in the blend	Swelling in $CHCl_3$[b]
		Fraction of PMMA-*g*-PA and unreacted PA[c]	Fraction of unreacted f-PMMA[d]			
80/20	PMMA**1**	52	48	40	27	b,w
	PMMA**2**	72	28	65	24	b,t
	PMMA**3**	40	60	25	23	b,w
70/30	PMMA**1**	72	28	60	21	b,w
	PMMA**2**	86	14	80	24	1.45,t
	PMMA**3**	70[e]	30[e]	54[e]	23	b,w
60/40	PMMA**1**	–	–	–	–	–
	PMMA**2**	94	6	90	30	1.35,t
	PMMA**3**	94[e]	6[e]	90[e]	22	b,w

[a] Ratio (wt%) of f-PMMA non-dissolved in chloroform over total amount of f-PMMA in the blend.
[b] Aspect of the samples after 72 h in chloroform at room temperature (b, the extrudate breaks; w, the extrudate turns white; t, the extrudate remains transparent and the numerical values correspond to the ratio of the sections after and before swelling).
[c] Fraction (wt%) non-soluble in chloroform.
[d] Fraction (wt%) soluble in chloroform.
[e] The amount of grafted PMMA**3** chains is overestimated [22]. As a result, the amount of PMMA**3**-*g*-PA + unreacted PA is overestimated and the amount of unreacted PMMA**3** chains is underestimated.

of PA content for the blends based on PMMA**2** is displayed in Fig. 4. Pictures A, B and C correspond to annealed samples containing, respectively, 20, 30 and 40 wt% PA. For the sake of comparison, the morphology of the 70/30 blend prior to annealing is presented in Fig. 4(D). Upon increasing PA content, the amount of graft copolymer in the blend increases (see also Fig. 3), PA domains disappear and the concentration of bilayers increases. The blends self-assemble into a swollen lamellar phase. Extraction of unreacted PMMA**2** enhances the lamellar morphology of the system. Fig. 5 illustrates this for the PMMA**2**/PA blend after extraction (initial composition 70/30), which has an average lamellar spacing estimated at 40 nm by SAXS

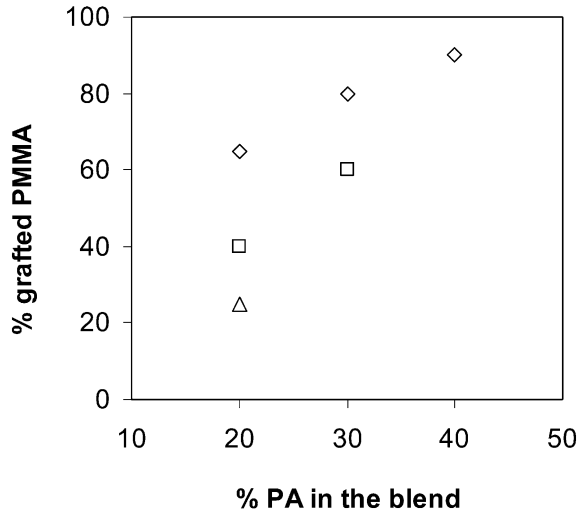

Fig. 3. Amount of grafted PMMA as a function of the amount of PA in the blend for (□) PMMA**1**, (◇) PMMA**2** and (△) PMMA**3** [22].

experiments. This sample is expected to contain mainly graft copolymer and a low amount of unreacted PA.

3.3. Blends properties

Adding some polyamide to PMMA leads to materials with improved properties compared to pure PMMA. For instance, the extrudates were immersed in chloroform to investigate solvent resistance of the blends. The results are listed in Table 2. Note that the aspect of the samples does not change even after several months in solvent. None of the blends is soluble in chloroform due to the presence of the graft copolymer. Graft copolymers can yield to connectivity of PA domains through molecular bridging or help to stabilize co-continuous structure [6]. Blends of PMMA**2** and PA remain transparent and, above 30 wt% PA, the specimens do not break but swell homogeneously. The swelling ratio decreases when the amount of PA increases. The other blends turn white and break as the solvent swells f-PMMA domains. Solvent resistance clearly depends on the system self-assembly and on the amount of graft copolymer formed during blending.

Blends of PMMA**2** and PA also exhibit interesting thermomechanical properties. The evolution of storage modulus and $\tan\delta$ as a function of temperature are displayed in Fig. 6(A) and (B), respectively. Unlike the non reactive system (data not shown), reactive blends do not creep above the glass transition of PMMA but exhibit a plateau of storage modulus till the melting point of PA close to 220 °C. The plateau arises from the connectivity of crystalline PA domains throughout the specimens which reinforces the materials. Increasing the amount of PA in the blends leads to better creep resistance arising from a higher

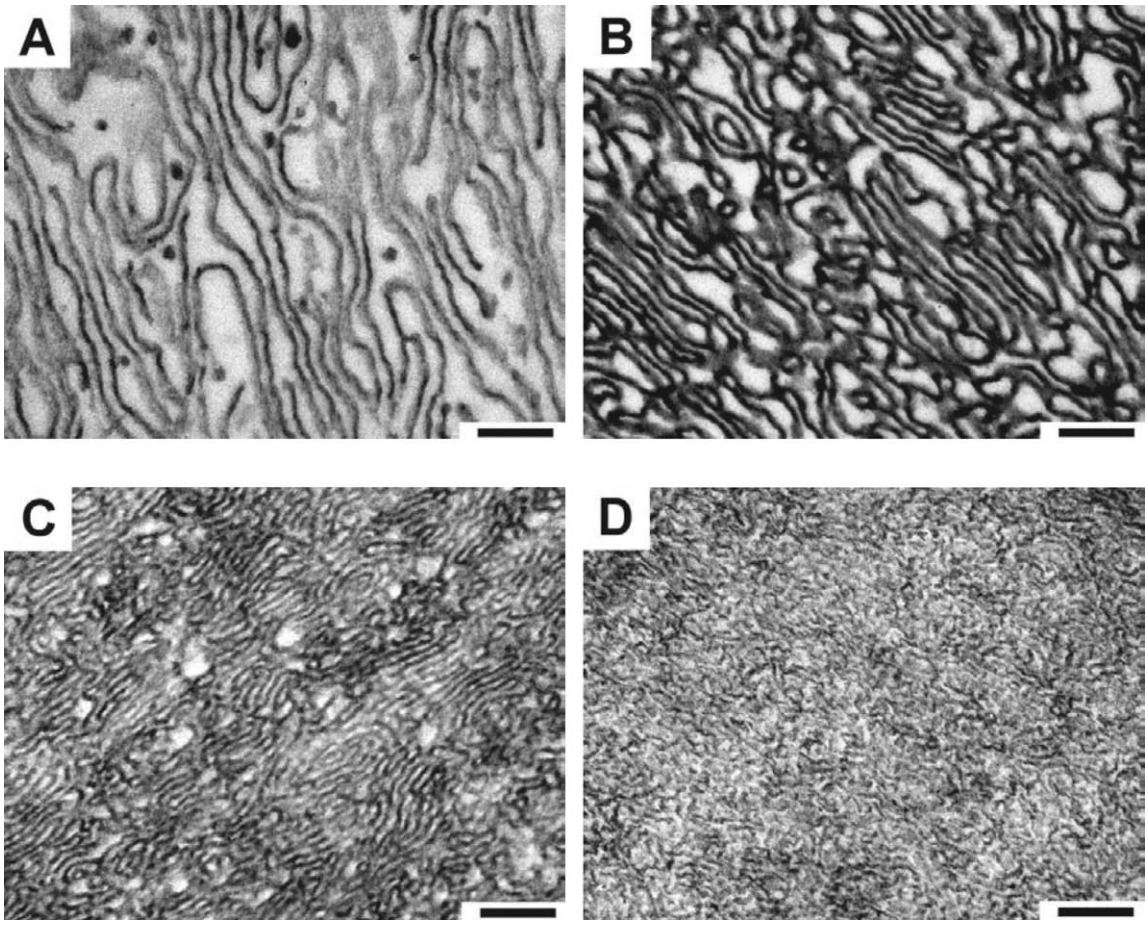

Fig. 4. TEM micrograph of the different PMMA**2**/PA blends after 20 h of annealing at 225 °C: (A) 80/20, (B) 70/30 and (C) 60/40 and TEM micrograph of (D) 70/30 PMMA**2**/PA extrudate, (sliced perpendicular to the original flow direction). Scaling bars correspond to 200 nm.

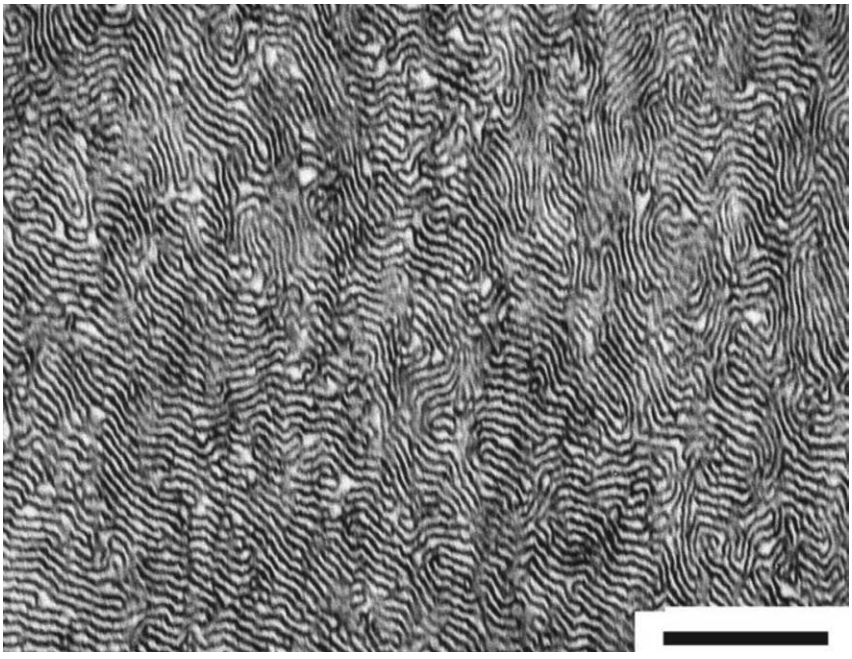

Fig. 5. TEM micrograph of the 70/30 PMMA**2**/PA blend after selective extraction of unreacted PMMA**2** followed by annealing at 225 °C for 20 h. The scale corresponds to 500 nm.

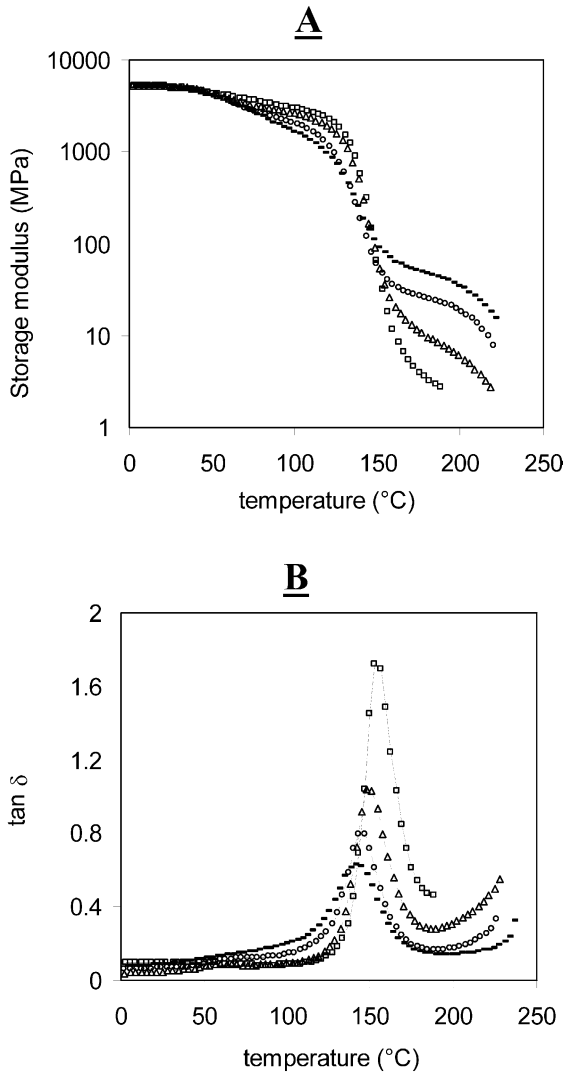

Fig. 6. Temperature dependence of storage modulus (A) and tan δ (B) of (□) PMMA**2** and PMMA**2**/PA blends: (△) 80/20, (○) 70/30, (–) 60/40.

fraction of graft copolymer in the blend. The curves corresponding to the blends, presented in Fig. 6(A), exhibit a slight decrease in the storage modulus close to 50 °C which corresponds to T_g of polyamide and a second one at higher temperature corresponding to T_g of PMMA**2**. The evolution of tan δ displayed in Fig. 6(B) reveals that T_g of PMMA**2** shifts to lower temperature with increasing amount of PA in the blend. T_g decreases from 154 °C for pure PMMA**2** to 152, 144 and 140 °C for the blends with 20, 30 and 40 wt% PA, respectively. No significant broadening of tan δ peak with increasing amount of PA was observed. Such shifts of T_g of the hard phase were already observed in neat copolymers [24]. They result from the cooperative softening induced by the soft phase close to the interface, in our case by the short amorphous PA chains. The shift in T_g of PMMA**2** may also result from the chemical modification of the backbone as cyclic imide functions with a pendant group are introduced during blending [25].

The ability of PA to crystallize when confined in nanodomains was also verified by DSC experiments. The degree of crystallinity of each blend is given in Table 2. It never reaches the value of pure PA6 (measured at 35%) but remains between 21 and 30%. The difference can be attributed to confinement of PA chains in self-assembled nanodomains and to a difference of mobility between grafted and free PA chains that can disturb the crystallization process.

4. Discussion and conclusion

Blending experiments on the system f-PMMA/short PA suggest that the density of reactive groups on the PMMA backbone govern the morphology and the stability of the blend. The graft copolymers obtained in this study are expected to be quite complex. Once a f-PMMA chain attaches a PA graft and if the reaction proceeds quickly, the polymer will preferably stay at the interface for further grafting on the neighboring groups than being expelled [26]. Grafting will thus not proceed homogeneously, part of the f-PMMA chains never reaching the interface and remaining ungrafted in the final blend. The structure of the graft copolymer is expected to vary with the density of reactive groups on f-PMMA chains (PMMA**1**, PMMA**2** and PMMA**3** have on average 2, 24 and 30 anhydride units randomly distributed along the backbone, respectively) and with the composition of the blends.

As PMMA**1** bears only a few reactive groups, PMMA**1**-*g*-PA copolymer is expected to have only a few grafts and to stabilize an interface with a strong curvature towards polyamide. As the density of reactive units increases, the distance between grafts decreases, leading to a smaller mean curvature and, ultimately, a flat interface (almost zero mean curvature) which corresponds to PMMA**2**-*g*-PA self-assembly. This evolution is schematically displayed in Fig. 7. When grafting density further increases, curvature should reverse and the interface should be curved towards PMMA, as presented in Fig. 7. This seems to correspond to PMMA**3**-*g*-PA. Note that the evolution of the mean curvature described in Fig. 7 is only schematic and does not necessarily fit the actual mean curvature of the aggregates formed by the PMMA-*g*-PA copolymers.

As we saw previously, pure graft copolymer is never achieved for this system (Fig. 3). The incorporation of remaining homopolymers in the self-assembly will depend on the graft density of the copolymers. When the graft density is too high, both PA grafts and PMMA loops (PMMA segments between grafts) are stretched and tend to expel unreacted homopolymers from the interface [14]. This seems to occur in PMMA**3**/PA blends (Fig. 2(F)). Note that in this system, the average distance between anhydride groups on PMMA**3** is shorter than the PA graft. On the other extreme, in PMMA**1**/PA blends, PMMA**1**-*g*-PA copolymers have a low graft density and form aggregates with extended PMMA loops and a strong curvature toward PA. The blend

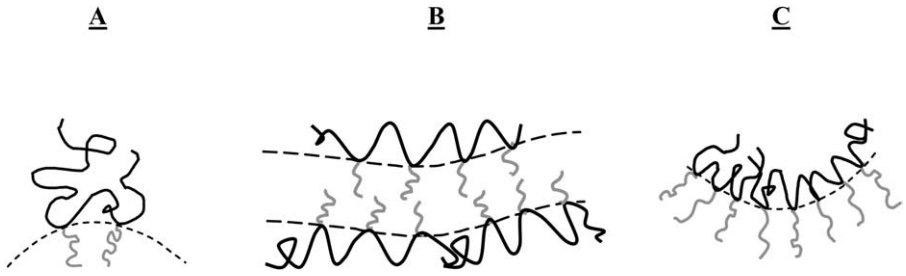

Fig. 7. Schematic representation of the self-assembly of PMMA-*g*-PA as a function of PA graft density, which increases from A to C, and can be compared to the evolution of the graft copolymers: PMMA**1**-*g*-PA, PMMA**2**-*g*-PA and PMMA**3**-*g*-PA. Chains of PMMA are in black and chains of PA are in grey.

forms a stable fine dispersion of PA domains in the PMMA**1** matrix (Fig. 2(D)). However, strong curvature of the interface leads to limited solubility of PA chains and thus to inhomogeneous dispersion [16,17]. Finally, PMMA**2**/PA blends seem to correspond to an optimum case. PMMA**2**-*g*-PA copolymers stabilize a flat interface, can incorporate unreacted homopolymers [15,16] and allow the system to reach high conversion of grafting. Note that inherent polydispersity of such graft copolymers (molar mass of f-PMMA and PA, distribution of reactive groups along the f-PMMA backbone, as well as randomness in attachment of the grafts) allows local fluctuations of the curvature, which seem to be favorable to the swelling of the lamellar-like phase by unreacted chains [6].

Superior properties of PMMA**2**/PA blends with 30 wt% or more PA (solvent and creep resistance) may be attributed to the high amount of graft copolymer formed during reactive blending and the resulting opportunity to form molecular bridges between PA nanodomains. Co-continuity of the blended morphologies (Fig. 4(D)) further helps to improve connectivity. Swollen lamellar morphology obtained upon annealing are therefore most likely interconnected.

The molar ratio anhydride/amine for all the blends is listed in Table 3. One would expect to find increasing efficiency of grafting with increasing f-PMMA functionality. However, our data clearly show an optimum of grafting for the blends based on PMMA**2**. Despite the large excess of anhydride in PMMA**3**/PA blends, a non-negligible amount of PA remains free (Fig. 2(F)). We attribute this feature to the tendency of the highly grafted PMMA**3**-*g*-PA copolymer to expel unreacted PMMA**3** and PA chains. PMMA**3**-*g*-PA copolymers formed during the first step of blending accumulate between PMMA**3** and PA phases, inhibiting further reaction between PMMA**3** and PA chains.

Table 3
Anhydride/amine molar ratio

% PA in the blend	Stoichiometric ratio anhydride/amine for		
	PMMA**1**/PA	PMMA**2**/PA	PMMA**3**/PA
20	0.5	5.7	7.2
30	0.3	3.3	4.2
40	–	2.1	2.7

The results reported here show that it is possible to achieve almost transparent PMMA/PA blends by reactive blending even if the blends include a semi-crystalline component. Annealing reveals that the morphology is not at equilibrium at the end of the blending process. We found that the efficiency of the graft copolymers to stabilize the blends is related to their structure. Furthermore, there is a correlation between optimum grafting and functionality of the backbone. These points are under further investigation in our group. Finally, nanostructured blends exhibit unique properties related to their self-assembly (solvent resistance, increased creep resistance up to 200 °C).

Acknowledgements

The authors gratefully acknowledge ARKEMA, CNRS and ESPCI for financial support. We thank A. Bonnet for helpful discussions, M. Millequant and J. Lescec for SEC characterization, and S. Girault for helpful discussion and comments on the manuscript. M.F. would like to acknowledge P. Coupard for help with TEM experiments.

References

[1] Koning C, Van Duin M, Pagnoulle C, Jerome R. Prog Polym Sci 1998;23:707.
[2] Orr CA, Adedeji A, Hirao A, Bates FS, Macosko CW. Macromolecules 1997;30:1243.
[3] Charoensirisomboon P, Inoue T, Weber M. Polymer 2000;41:6907.
[4] Yin C, Koulic C, Pagnoulle C, Jerome R. Macromolecules 2001;34:5132.
[5] Steurer A, Hellmann GP. Polym Adv Technol 1998;9:297.
[6] Pernot H, Baumert M, Court F, Leibler L. Nat Mater 2002;1:54.
[7] Koulouri EG, Kallitsis JK, Hadziioannou G. Macromolecules 1999;32:6242.
[8] Orr CA, Cernohous JJ, Guegan P, Hirao A, Jeon HK, Macosko CW. Polymer 2001;42:8171.
[9] Yin Z, Koulic C, Jeon HK, Pagnoulle C, Macosko CW, Jerome R. Macromolecules 2002;35:8917.
[10] Jeon HK, Macosko CW, Moon B, Hoye TR, Yin Z. Macromolecules 2004;37:2563.
[11] Lyu SP, Cernohous JJ, Bates FS, Macosko CW. Macromolecules 1999;32:106.
[12] Yin C, Pagnoulle C, Jerome R. Langmuir 2003;19:453.

[13] Jiao J, Kramer EJ, De Vos S, Möller M, Koning C. Macromolecules 1999;32:6261.
[14] de Gennes PG. Macromolecules 1980;13:1069.
[15] Leibler L. Makromol Chem-M Symp 1988;16:1.
[16] Matsen MW. Macromolecules 1995;28:5765.
[17] Janert PK, Schick M. Macromolecules 1997;30:137.
[18] Gido SP, Lee C, Pochan DJ, Pispas S, Ways JW, Hadjichristidis. Macromolecules 1996;29:7022.
[19] Hallden-Abberton M. Polym Mater Sci Eng 1993;68:245 [see also p. 249].
[20] Jamieson A, McNeill IC. Eur Polym J 1974;10:217.
[21] Liberti FN, Wunderlich BJ. J Polym Sci, Part A-2 1968;6:833.
[22] TEM experiments, not displayed here, on extrudates after selective extraction reveal that no f-PMMA remains in the blends except for blends of PMMA**3** with 30 and 40 wt% of PA. The values for the relative amount of grafted f-PMMA given in the Table 2 are therefore overestimated in these cases and the corresponding points are not represented in Fig. 3.
[23] A complete characterization of the blends by size exclusion chromatography is now in progress. The data indicate that the annealing process induces a variation of the amount of grafted PA of less than 10%.
[24] Morese-Seguela B, St-Jacques M, Renaud JM, Prud'homme J. Macromolecules 1980;13:100.
[25] Vermeesch I, Groeninckx. J Appl Polym Sci 1994;53:1365.
[26] Yin Z, Koulic C, Pagnoulle C, Jerome R. Macromol Symp 2003;198:197.